ISSN 1063-7834, Physics of the Solid State, 2015, Vol. 57, No. 11, pp. 2286–2289. © Pleiades Publishing, Ltd., 2015.
Original Russian Text © A.S. Oreshonkov, A.K. Khodzhibaev, A.S. Krylov, M.F. Umarov, A.N. Vtyurin, 2015, published in Fizika Tverdogo Tela, 2015, Vol. 57, No. 11, pp. 2218–2221.

Raman Spectroscopy Study of the Behavior of the Soft Mode in a Structural Phase Transition in the $Pr_3Sb_5O_{12}$ Crystal

A. S. Oreshonkov[a, b, *], **A. K. Khodzhibaev**[c], **A. S. Krylov**[a, b], **M. F. Umarov**[d], **and A. N. Vtyurin**[a, b]

[a] *Kirensky Institute of Physics, Siberian Branch of the Russian Academy of Sciences,*
Akademgorodok 50–38, Krasnoyarsk, 660036 Russia
[b] *Siberian Federal University, pr. Svobodnyi 79, Krasnoyarsk, 660041 Russia*
[c] *Khujand State University, pr. Mavlonbekov 1, Khujand, Tajikistan*
[d] *Volgograd State University, Universitetskii pr. 100, Volgograd, 400062 Russia*
** e-mail: oreshonkov@ihp.krash.ru*

Received April 14, 2015

Abstract—The structural phase transition in the $Pr_3Sb_5O_{12}$ crystal has been studied using Raman spectroscopy. The phase transition is accompanied by the recovery of the soft mode below $T = 735$ K, which is associated with the displacements of the oxygen and antimony atoms.

DOI: 10.1134/S1063783415110256

1. INTRODUCTION

One of the natural minerals containing antimony is antimonite. The largest deposit of antimony “Skal’noe” contains more than 50% of the antimony reserves of the CIS, with the antimony content in the concentrate up to 60%. According to the confirmed reserves of antimony, Tajikistan occupies the first place in the CIS and the third place in Asia, after China and Thailand [1]. Studies of compounds of the antimonite family, apart from fundamental interest, have applied value.

In the last decades, new compounds of the antimonite family [2–4] were synthesized based on antimony oxides, namely, $R_3Sb_5O_{12}$ (R is a rare-earth metal), in which ferroelectric and piezoelectric properties were revealed [5, 6]. The structure of the unit cell of crystals of this family at room temperature is shown in Fig. 1 (space group $I\bar{4}3m$, $Z = 4$ [3]). As is seen from Fig. 1, rare-earth cations are surrounded by eight oxygen anions; i.e., they are located in eight-vertex polyhedra, which represent a distorted “folded (Thomson) cube.” These polyhedra are joined by common edges and form a three-dimensional framework whose holes are occupied by Sb atoms.

As the temperature increases, crystals of this family undergo a structural phase transition to the centrosymmetric cubic phase $Im3m$. In $Nd_3Sb_5O_{12}$, $Gd_3Sb_5O_{12}$, and $Er_3Sb_5O_{12}$, these transitions were observed at 723, 713, and 643 K, respectively [7]. The temperature dependences of the permittivity of $R_3Sb_5O_{12}$ (R = Pr, Nd, Gd, Er) were studied in [8]. It was shown that, for the $Pr_3Sb_5O_{12}$ crystal, the permittivity $\varepsilon(T)$ has a maximum at 735 K, which can also indicate a phase transition in this temperature range. An assumption about the existence of this transition was also made earlier in [9].

Raman spectroscopy is traditionally used to study structural instabilities of crystals. The Raman spectra of $Pr_3Sb_5O_{12}$ crystals at room temperature were obtained earlier in [10]. However, their temperature dependence was not studied.

Therefore, the purpose of this work was to perform a Raman spectroscopy study of structural phase transitions in the $Pr_3Sb_5O_{12}$ crystal over a wide tempera-

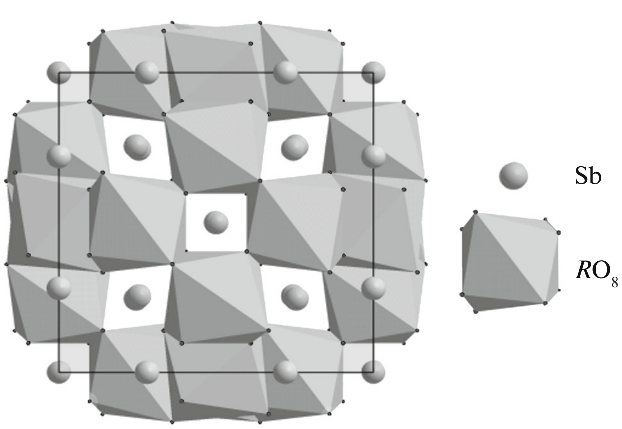

Fig. 1. Structure of the $Pr_3Sb_5O_{12}$ crystal at room temperature.

ture range, including the region of the presumed phase transition.

2. EXPERIMENTAL TECHNIQUE

The Raman spectra were excited by polarized radiation from a helium–neon laser at a wavelength of 632.8 nm and a power of 50 mV. The spectra in a 90° geometry were measured on a DFS-24 spectrometer with a spectral slit width of 0.5 cm^{-1} in the frequency range of 20–1200 cm^{-1} [11]. For temperature investigations, we use a high-temperature thermostat [12], which made it possible to perform measurements in the temperature range of 300–800 K. The thermal stabilization of the sample during the recording of the spectrum was no worse than 0.1 K. The samples to be studied had the form of parallelepipeds 3 × 4 × 6 mm in size. The samples did not contain defects or inclusions visible in a microscope. Their high quality was also confirmed by measurements of the acoustic Q factor.

To obtain quantitative values of the positions and widths of spectral lines upon the decomposition of the experimental spectrum into components, the shape of the Lorentzian profile is usually used, as in [13, 14]:

$$I_L(A,\omega,\Gamma) = \frac{2}{\pi}\frac{I\Gamma}{4(x-\omega)^2+\Gamma^2}, \qquad (1)$$

where A is the intensity, ω is the frequency (cm^{-1}), Γ is the line half-width, and x is the frequency (the current coordinate in the decomposition, cm^{-1}). A more correct approach in the description of the low-frequency region of the spectrum (<150 cm^{-1}) is the use of the damped harmonic oscillator (DHO) function [15] as the fitting function.

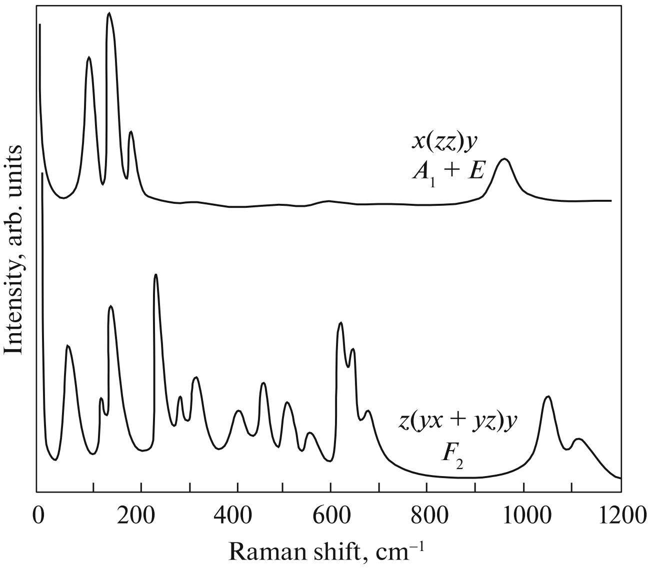

Fig. 2. Raman spectra of $\mathrm{Pr_3Sb_5O_{12}}$ in the scattering geometries $x(zz)y$ and $z(yx + yz)y$.

$$I_{\mathrm{DHO}}(A,\omega,\Gamma) = F(x,T)\frac{2I\omega^2\Gamma x}{(\omega^2-x^2)^2+4\Gamma^2x^2}. \qquad (2)$$

Here,

$$F(x,T) = \begin{matrix} n(\omega)+1 & (\text{Stokes part}) \\ n(\omega) & (\text{anti-Stokes part}), \end{matrix} \qquad (3)$$

$$n(\omega,T) = \left[\exp\left(\frac{\hbar\omega c}{k_{\mathrm{B}}T}\right)-1\right]^{-1}, \qquad (4)$$

where $\hbar$ is the Planck constant, c is the light velocity, and k_{B} is the Boltzmann constant.

In this case, the frequency of the effective soft mode is described by the following expression [15]:

$$\omega_S = \sqrt{\omega^2-\Gamma^2}. \qquad (5)$$

Since, at high values of ω, the spectral parameters obtained as a result of the expansion by the Lorentzian function and the damped harmonic oscillator function coincide, the entire spectral range is described by the DHO function.

3. RESULTS AND DISCUSSION

In the $I\bar{4}3m$ phase, the expansion of the vibrational representation at the center of the Brillouin zone has the form

$$\begin{aligned}\Gamma_{\mathrm{vibr}}(I\bar{4}3m) &= 6A_1(xx,yy,zz)+3A_2 \\ &+ 9E(xx,yy,zz)+13F_1+18F_2(xy,xz,yz).\end{aligned} \qquad (6)$$

The parenthetic quantities are the Raman tensor components, in which the corresponding vibrational excitations are active. For polar modes F_2, we can also expect the splitting into LO–TO doublets [10]. In the presumed high-temperature phase, the corresponding expansion has the form

$$\begin{aligned}\Gamma_{\mathrm{vibr}}(Im3m) &= 3A_{1g}(xx,yy,zz) \\ &+ 2A_{2g}+5E_g(xx,yy,zz) \\ &+ 6F_{1g}+7F_{2g}(xy,xz,yz)+A_{1u} \\ &+ 3A_{2u}+4E_u+7F_{2u}+11F_{1u}.\end{aligned} \qquad (7)$$

The spectrum of the $\mathrm{Pr_3Sb_5O_{12}}$ crystal ($T = 300$ K) in the scattering geometries $x(zz)y$ and $z(yx + yz)z$ is shown in Fig. 2. At that, in the geometry $x(zz)y$, the A_1 and E modes are active, whereas in the geometry $z(yx + yz)z$, only the F_2 modes are active. The number of observed lines is substantially less than that allowed by the selection rules, which, probably, is associated with their rather large widths at room temperature and with the significant overlap.

The transformation of the Raman spectrum in the geometry $x(zz)y$ with an increase in the temperature is shown in Fig. 3. Heating of the crystal leads to a fur-

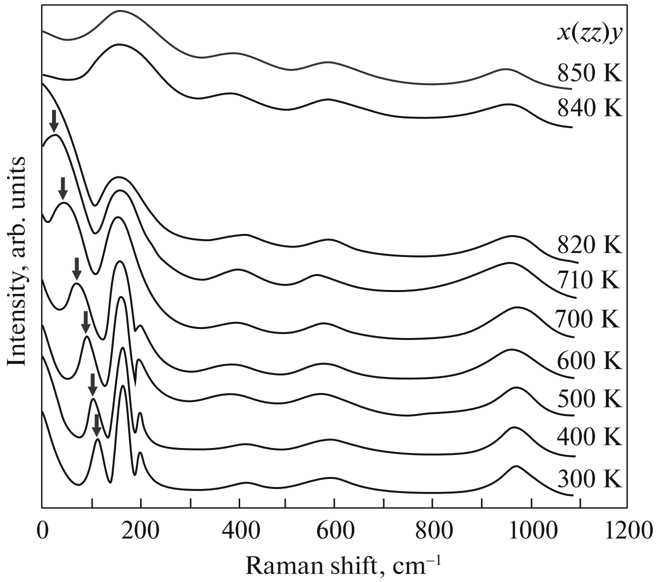

Fig. 3. Transformation of the Raman spectrum of the $Pr_3Sb_5O_{12}$ crystal with a decrease in the temperature.

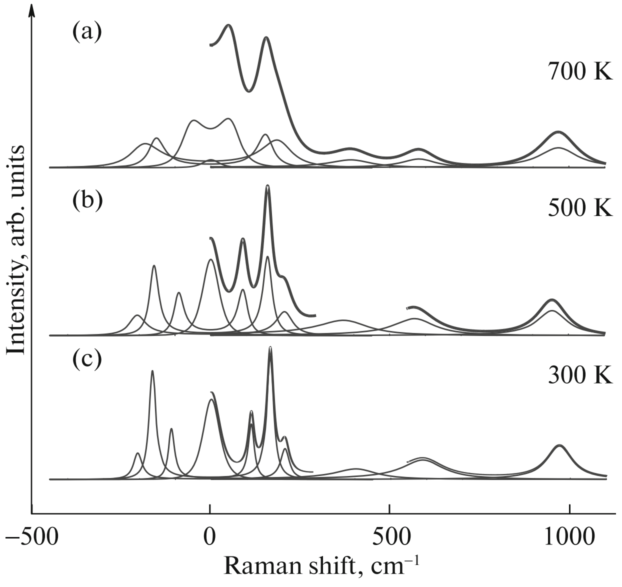

Fig. 4. Structure of the Raman spectrum of the $Pr_3Sb_5O_{12}$ crystal at temperatures $T =$ (a) 700, (b) 500, and (c) 300 K. Thin lines show the decomposition of the spectral profile into components with the use of the DHO function.

ther increase in the line width. Above the temperature of the presumed transition, according to the selection rules, the number of lines decreases.

An important feature was found in the spectrum of the diagonal component $x(zz)y$ (Fig. 3). As the transition point is approached, the low-frequency line at 114 cm^{-1} and $T = 300$ K begins to rapidly shift toward the Rayleigh edge.

Figure 4 shows the decomposition of the spectral profile in the diagonal component $x(zz)y$ at temperatures of 300, 500, and 700 K with the use of the DHO function. The spectral region below 250 cm^{-1} is described by three profiles.

The behavior of the square of the frequency (5) of this line (Fig. 5) shows that, in a wide range below the transition point, there is a linear dependence on the temperature, which is typical of the soft mode. The extrapolation of this dependence to zero gives the critical temperature of 735 K, which agrees well with the previously observed [8] temperature of the maximum permittivity and corresponds to a second-order transition.

A group-theoretical analysis of the eigenvectors of normal vibrations in the $I\bar{4}3m$ phase shows that, in the totally symmetric lattice vibrations of this mode, the O and Sb ions participate; i.e., the transition is associated with displacements of these ions. This, in particular, can explain the weak dependence of the transition temperature on the type of rare-earth ion.

Above the transition, there is no condensation of the soft mode. The group-theoretical analysis shows that the transition from the presumed high-temperature phase $Im3m$ to the phase $I\bar{4}3m$ is described by the irreducible representation $\tau_4(\kappa_{11}) - A_{2u}$, according to which the one-component order parameter is transformed [8]. Modes of this symmetry are inactive in optical vibration spectra.

Attention is drawn to the fact that the large (more than 10 cm^{-1}) width of all the Raman lines is observed not only near the transition point, but also in a wide

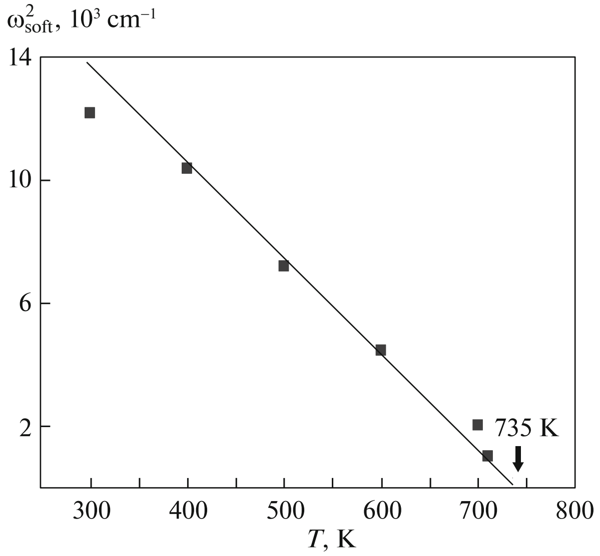

Fig. 5. Temperature dependence of the square of the frequency of the soft mode. The linear dependence corresponds to the behavior in the second-order phase transition.

temperature range up to room temperature. This can point to a considerable anharmonicity of lattice vibrations of the studied crystal and anomalously high amplitudes of vibrations of the ions displaced during the transition. Probably, the crystal lattice remains partly disordered also below the transition and one more structural phase transition at lower temperatures is not excluded.

4. CONCLUSIONS

Thus, the studied phase transition at 735 K in the $Pr_3Sb_5O_{12}$ crystal is a second-order transition of the displacive type with the soft lattice mode clearly observed in the distorted phase. The observed phase transition is associated with the displacements of the oxygen and antimony ions.

ACKNOWLEDGEMENTS

The study was supported in part by the Ministry for Education and Science of the Russian Federation.

REFERENCES

1. R. D. Bakhtdavlatov, Gorn. Zh. **S2**, 22 (2012).
2. Kh. M. Kurbanov, M. N. Tseitlin, R. Ch. Bichurin, V. I. Popolitov, and S. Yu. Stefanovich, Dokl. Akad. Nauk Resp. Tadzh. **24**, 494 (1981).
3. Kh. M. Kurbanov, N. B. Butikova, A. G. Gukalova, and V. P. Glyakin, Dokl. Akad. Nauk SSSR **281**, 1119 (1985).
4. A. G. Gukalova, V. P. Glyakin, and M. N. Tseitlin, Koord. Khim. **13**, 918 (1987).
5. M. F. Umarov, A. N. Vtyurin, and A. K. Khodzhibaev, in *Proceedings of the 13th International Symposium "Order, Disorder and Properties of Oxides" (ODPO-13), Rostov-on-Don, September 16–21, 2010*, p. 178.
6. M. F. Umarov, K. S. Koziev, and A. K. Khodzhibaev, Uch. Zap. Khudzhanskogo Gos. Univ. im. Akad. B. Gafurova **2**, 58 (2012).
7. Kh. M. Kurbanov, M. N. Tseitlin, and I. P. Raevskii, Izv. Akad. Nauk SSSR, Neorg. Mater. **20**, 1199 (1984).
8. M. F. Umarov, A. K. Khodzhibaev, K. S. Koziev, and S. Sh. Akhmedov, Vestn. Tadzh. Nats. Univ. **106**, 150 (2013).
9. V. P. Glyakin, Candidate's Dissertation (Institute of Physics, Siberian Branch of the Academy of Sciences of the USSR, Krasnoyarsk, 1989).
10. I. L. Botto, E. J. Baran, C. Cascales, I. Rasines, and R. Saez Puche, J. Phys. Chem. Solids **52**, 431 (1991).
11. M. F. Umarov, A. K. Khodzhibaev, and K. S. Koziev, Vestn. Tadzh. Nats. Univ. **106**, 97 (2013).
12. Z. M. Rakhmatova, M. F. Umarov, and A. K. Khodzhibaev, Vestn. Tadzh. Tekh. Univ. im. Akad. M.S. Osimi **22**, 4 (2013).
13. V. K. Malinovsky, A. M. Pugachev, and N. V. Surovtsev, Phys. Solid State **50** (6), 1137 (2008).
14. A. S. Krylov, E. M. Merkushova, A. N. Vtyurin, and L. I. Isaenko, Phys. Solid State **54** (6), 1275 (2012).
15. H. Taniguchi, M. Itoh, and D. Fu, J. Raman Spectrosc. **42**, 706 (2011).

Translated by E. Borisenko